DEVELOPMENT OF NOVEL METAPOROUS STRUCTURE AT LOW-MID FREQUENCY FOR AIRBORNE COMPRESSOR NOISE OF AN ELECTRICAL VEHICLE

BARIŞ VATANSEVER

ÖZYEĞİN UNIVERSITY

DECEMBER, 2024

DEVELOPMENT OF NOVEL METAPOROUS STRUCTURE AT LOW-MID FREQUENCY FOR AIRBORNE COMPRESSOR NOISE OF AN ELECTRICAL VEHICLE

by
Barış Vatansever

Thesis
Submitted in Partial Fulfillment of the
Requirements for the Degree of

Master of Science

in
Mechanical Engineering

Advisor: Assoc. Prof. Polat Şendur
Co-Advisor: Dr. Aydın Özcan

Graduate School of Science and Engineering
Özyeğin University
İstanbul

December, 2024

DEVELOPMENT OF NOVEL METAPOROUS STRUCTURE AT LOW-MID FREQUENCY FOR AIRBORNE COMPRESSOR NOISE OF AN ELECTRICAL VEHICLE

Approved by:

Assoc. Prof. Polat Şendur, Advisor
Department of Mechanical Engineering
Özyeğin University

Asst. Prof. Ramazan Ünal
Department of Mechanical Engineering
Özyeğin University

Prof. Çetin Yılmaz
Department of Mechanical Engineering
Boğaziçi University

Approval Date: November 28, 2024

To my family

DECLARATION OF ORIGINALITY

I hereby declare that I am the sole author of this thesis and that this is the true copy of my thesis, including the final revisions, approved by my thesis committee. All data and information have been obtained, produced, and presented in accordance with the rules of research ethics and principles of academic honesty. As required by these rules, to the best of my knowledge I have acknowledged ideas, thoughts, and any copyrighted material in accordance with the standard referencing rules. I certify that any part of this thesis has not been submitted for a degree or diploma in another educational institution.

Barış Vatansever

ABSTRACT

Metamaterials have gained an increasing attention as a way of absorbing noise to achieve improved acoustic performance on vehicles, and thanks to their novel functionalities compared to traditional designs, these structures are employed by many automotive companies as noise-reduction solutions for engineering applications. One of the key challenges for automotive original equipment manufacturers (OEMs) in the noise, vibration, and harshness (NVH) development process is absorption performance in the frequency range of 400 Hz to 800 Hz. Although sound engineers use porous polyurethane in these frequency ranges, the absorption performance of these designs is limited to meet increasing customer expectations. Besides, managing airborne noise in vehicles is particularly challenging in the low frequency spectrum. The main purpose of this study is to develop a metaporous sound barrier incorporating a Helmholtz resonator, effective in the low to mid-frequency range of the spectrum. For this purpose, a frequency domain simulation was carried out to obtain the absorption coefficient, analyze frequency-dependent effects, and identify critical frequencies in vehicle acoustics. Furthermore, local resonance effects to prevent acoustic waves were investigated and design parameters of metastructure were analyzed using a multiphysics-based simulation model. These results were validated experimentally using an acoustic impedance tube. The methodology is demonstrated in a battery electric vehicle (BEV) to improve airborne compressor noise during motor idling. The optimum design parameters were determined using the Taguchi design method. Finally, the performance of developed metaporous material was validated through vehicle-level tests, with results showing an improvement of 3 dB(A).

Keywords: Metamaterial, NVH, low-mid frequency, exterior noise, Taguchi design method

ÖZET

Metamalzemeler, araçlarda gelişmiş akustik performansı elde etmek için gürültüyü absorbe etmenin yolundan biri olarak literatürde daha fazla kabul görüyor ve geleneksel tasarımlara göre yapıların yeni fonksiyonları ön plana çıkıyor. Birçok otomotiv firması tarafından mühendislik uygulamalarında gürültü azaltma çözümü olarak kullanılmaktadır. Gürültü, titreşim ve sertlik (NVH) geliştirme sürecinde otomotiv orjinal ekipman üreticilerinin (OEM'ler) karşılaştığı temel zorluklardan biri 400 ile 800 Hz arasındaki gürültüyü absorbe etme performansının zor olmasıdır. Ses mühendisleri bu frekans aralıklarında gözenekli poliüretan malzemeler kullansalar da bu tasarımların absorbe etme performansı artan müşteri beklentilerini karşılamada yetersiz kalmaktadır. Ayrıca Helmholtz rezonatörlerinin yaygın olarak kullanıldığı düşük frekans spektrumunda araçlarda hava kaynaklı gürültüyü yönetmek ve engellemek oldukça zordur. Bu çalışmanın esas amacı spektrumun düşük-orta frekans aralığında etkin olan Helmholtz rezonatörün kullanıldığı meta gözenekli kompozit bir ses bariyeri geliştirmektir. Bu amaçla akustik dalgaları önlemeye yönelik lokal rezonans etkileri araştırılmış ve Multifizik tabanlı bir simülasyon modeli kullanılarak metayapının tasarım parametreleri oluşturulmuştur. Metodoloji, elektrikli bir aracın (BEV) motor rölanti manevrası sırasında havadan yayılan kompresör gürültüsünün analizi yoluyla gösterilmiştir. Geliştirilen tasarımda optimum tasarım parametreleri Taguchi tasarım yöntemi kullanılarak belirlenmiştir. Sonlu eleman modellerinin sonuçları empedans tüpü ölçümleriyle doğrulanmıştır. Son olarak, geliştirilen meta gözenekli malzemenin performansı araç seviyesi testlerinde gerçekleştirildi ve sonuçlar motor rölantide halindeyken yaklaşık 3 dB(A) iyileşme göstermiştir.

Anahtar Kelimeler: Metamalzeme, Gürültü ve titreşim, düşük-orta frekans, dış gürültü, Taguchi tasarım metodu

ACKNOWLEDGEMENTS

This thesis was written as a result of collaboration between Ozyegin University and Türk Otomobil Fabrikası A.Ş. (TOFAŞ). Tofaş generously supported the manufacturing of the test specimens. The tests were carried out at Tofaş, Insulation laboratory tests and Semi Anechoic Room on Vehicle tests, and Acoustic Simulations were carried out at Ozyegin University, Vibrations and Acoustics Laboratory. First and foremost, I am indebted to Dr. Polat Sendur, my MSc supervisor, for his unwavering support, advise, excitement, and patience during my studies. He always advised me and encouraged and motivated me throughout my thesis research. His guidance aided me in completing the MSc requirements. I would also like to thank grande hero, Dr. Aydın Özcan who assisted and guided me as I researched my thesis and generously offered his significant expertise to me during my thesis and helped me to succeed in my MSc studies. Secondly, I want to express my gratitude to my friends, Aytekin Özkan and Mehdi Yıldız for helped me during prototype production and vehicle tests in NVH Research Laboratory and prototype department in TOFAŞ. Finally, I would like to express my gratitude to my wife and family. They supported me through all my difficulties and encouraged me to finish the thesis.

TABLE OF CONTENTS

LIST OF TABLES

LIST OF FIGURES

LIST OF ACRONYMS AND ABBREVIATIONS

NVH	: Noise, Vibration and Harshness
Hz	: Hertz
RMS	: Root Mean Square
EV	: Electric Vehicle
BEV	: Battery Electric Vehicle
ICE	: Internal Combustion Engine
HR	: Helmholtz Resonator
DPM	: Double Porosity Material
PU	: Polyurethane
A/C	: Air Conditioner
HVAC	: Heating, Ventilation, and Air Conditioning
ICP	: Integrated Circuit Piezoelectric
LMS	: Leuven Measurement Systems
SPL	: Sound Pressure Level
EFDM	: Equivalent Fluid Density Model
JCA	: Johnson–Champoux–Allard
FEM	: Finite Element Method
CFD	: Computational Fluid Dynamics
FRF	: Frequency Response Function
OEM	: Original Equipment Manufacturer
TOFAŞ	: Türk Otomobil Fabrikası A.Ş.
NACA	: National Advisory Committee for Aeronautics

1. INTRODUCTION

The literature review on the thesis is presented in Section 1.1, and the objectives are summarized in Section 1.2.

1.1 Literature Review

NVH product development is crucial for almost all means of transportation such as passenger cars and commercial vehicles [1]. In the automotive industry, suppliers work closely with the OEMs throughout the sound package development cycle to ensure the design meets customer expectations. NVH performance of a vehicle has an ever increasingly stronger impact on the customer perception of ride comfort and brand quality, and it has become one of the most prioritized attributes when purchasing a new car [2]. In the design process, NVH development is most commonly classified into powertrain NVH, road noise, wind noise and component noise [3]. For excitation frequencies below 400 Hz, vibrations coming from tire/road or from powertrain are transmitted by suspension mounts and excite the vehicle structure [4]. This leads an disturbing tonal noise that dominates the resulting noise spectrum between 180-300 Hz [5]. In this specified frequency (below 1000 Hz), there are limited specific studies in the literature and these consists of complex sound and vibration problems on motor accessory, for example, compressor noise problem. One of them is studied in terms of acoustic response of compressor, cavity resonances and shell vibration of the compressor by Dazhuang HE [6]. Sound engineers strive to reduce noise using conventional sound package solutions for both the interior and exterior noise of electric vehicles (EV) in the literature. For instance, to reduce the transmission of motor noise in EVs, the motor is packaged with double-layer sound package materials and the thickness and coverage of the sound package have a great impact on the optimization of the sound package [7, 8]. Another example is the proposed sound insulation hood for an air compressor unit, which aims to enhance blocking effect [9]. Therefore, an in-depth evaluation of EV accessories is necessary to comprehensively understand the NVH challenges of an electric vehicle [10]. The main sources of the noise from the outdoor unit are the structure-borne noise radiated from the chassis structure and airborne noise from the fan. The fan produces noise primarily at the blade passing frequency and its harmonics, which typically fall within the low-frequency range. Vibrations from the compressor is transmitted to the chassis structure through several paths, leading to noise radiation [11]. The effect of the compressor on exterior noise is even more pronounced in electric vehicles. Compressor noise generally falls within a relatively low-frequency range (500 and 630 Hz 1/3 octave band) [12] and is mainly due to the acoustic field pressure fluctuations excited by the movement of rigid mechanical parts [13]. As a result of these reasons, new NVH solutions are required for noise reduction in EVs. In the vehicle design cycle, it is customary to develop and optimize acoustic sound packages to improve interior noise and reduce external noise. A robust sound package design takes into account many design constraints, such as customer expectations, packaging envelope, and cost [14]. Sound package applications for vehicles with ICE are generally inadequate for EVs. To adapt these designs to EVs, the following challenges must be overcome [15]: i) motor high frequency tonal noise, ii)road noise and aerodynamic noise dominating the acoustic perception, necessitating the development of specialized sound packages distinct from those used for ICE vehicles, iii)exterior noise reduction for transparency. There have been many studies related to noise attenuation methods in the literature. For example, a theoretical method is employed to design acoustic barriers [16]. The attenuation of the sound pressure level depends on the distance from the sound source to the barrier, the dimension of the barrier, and the frequency spectrum of the sound source [16, 17]. In another study, radiated compressor noise is attenuated by using a sound curtain barrier wall made of fiberglass absorber bonded to a vinyl noise barrier around the compressor [18].

Helmholtz Resonators (HR) have found extensive applications in noise control, such as serving as low-frequency sound absorbers [19] or increasing the sound transmission loss of double wall partitions [20]. It has been recently demonstrated that acoustic metamaterials with Helmholtz resonators can exhibit promising applications for noise control. These findings open the possibility of developing various noise management applications or acoustic cloaks development [19, 21]. Acoustic metamaterials are materials with unusual properties that can change sound in unconventional ways and achieve effects that cannot be found naturally [22, 23]. In the literature, aluminum combined with porous metamaterials has been employed to enhance the viscous resistance and frictional effects of acoustic waves on the inner walls of the materials, resulting in the attenuation of sound energy [24]. Metamaterials have also been considered as one of the ideal materials in terms of noise absorption in the low frequency range [25, 26, 27]. Furthermore, different structures based on local resonance can effectively break through the technical bottleneck of low-frequency vibration and noise absorption [28, 29, 30, 31, 32, 33, 34]. They can control large-wavelength and low-frequency mechanical waves through sub-wavelength microstructures. Therefore, their use in acoustic applications is increasing, with applications spanning various fields [35, 36]. In one of the recent studies, a double porosity material (DPM) for low frequency sound absorption was proposed, significantly improving the sound absorption performance significantly around 450 Hz [37]. Acoustic metasurfaces with HR can generate a desired gradient through the tailoring of resonator structures and reflect the incident sound. The resulting metasurface can have superior properties, such as broad bandwidth, high transmission coefficient, well-matched acoustic impedance, and ease of fabrication [38, 39, 40]. In general, addressing low-frequency sound issues with conventional sound-package solutions can be quite challenging. From this perspective, metamaterials can be light-weight alternatives and their properties can be tuned for specific engineering applications. However, these metamaterials may incur higher product development costs due to complex fabrication processes. Additionally, they may only exhibit effective performance within a limited range of frequencies. Therefore, the design of metamaterials should be carefully engineered. In this study, the low frequency compression noise problem in BEV is considered. More specifically, the main objective of this research is to develop a sound barrier design aimed at attenuating compressor noise in a BEV in the frequency range of 400 Hz to 800 Hz for exterior noise. A new three-dimensional (3D) simulation model was developed as a Helmholtz resonator by combining metal and porous materials. The effects of various design parameters were explored using Taguchi design methodology, ultimately determining the best design parameters. The proposed design is validated on a physical prototype using an impedance tube test. Subsequently, the design is verified in vehicle-level tests while the vehicle is idling on A/C on condition.

1.2 Literature Objectives of the Thesis

The objectives of this thesis can be shown as developing a sound barrier design consisting of Aluminum walls with Helmholtz resonator by implementing a rigid baffle for better acoustic impedance and cavity and porous absorption material. This combination is verified with the help of virtual and experimental test results and parameter optimizations with Taguchi main effect method at the level of system and vehicle. This design is effective at low-mid frequency range of the spectrum in terms of compressor noise spectrum between 400 and 800 Hz and demonstrate metamaterial on the air borne compressor noise problem on exterior sound of amodel Battery Electric Vehicle(BEV). In the design phase, a model that generates a 3D model in ANSYS Spaceclaim has been identified from the literature. It has been analyzed in the frequency domain acoustic simulations in terms of the properties determined by literature article. The simulation results have been compared to the analytic data to obtain reliable simulation results in design phase developed. A new 3D Multiphysics model was then generated in terms of validated porous material. This design was investigated using Taguchi main effect method. It helped decide the optimum parameters of the design. Then, we produced a prototype using Aluminum part with the support of turning lathe. The vehicle's acoustic performance has been compared to new application on compressor without application with experimental tests. The compressor of the vehicle is covered with new design. Acoustic compressor noise test maneuvers are performed. They are compared under two conditions: with meta porous material and without meta porous material for the purpose of assessment the exterior noise level. Finally, the results have been demonstrated on BEV. Although all the methods mentioned above exist, the number of articles presented to the literature by combining the methods on vehicle is a few. The rest of the paper is organized as follows: The research problem is depicted in detail in Chapter 2. Details of analysis methodology are given in Chapter 3, including design methodology (Section 3.1), theoretical model (Section 3.2) and simulation model (Section 3.3). Optimization was detailed with the Taguchi design method (Section 4.1). The validation results of the proposed simulation model, using impedance tube tests validation, and vehicle level tests are presented in Chapter 5. Finally, conclusion and future works are given in Chapter 6 and Chapter 7 respectively.

2. PROBLEM DEFINITON

In this Chapter, problem definition on battery electric vehicle for the compressor air borne noise problem definition and describing experimental test equipment are presented in Section 2.1, and test results towards the air borne noise problem are presented in detail in Section 2.2.

2.1 Problem Definition on BEV for Compressor Noise

Electric compressors are typically driven either by the vehicle's primary electric drive system or by a separate electric motor dedicated to the air conditioning (A/C) system. Additionally, these compressors are used to control the temperature of the vehicle's battery pack system, which is crucial for the performance and longevity of the battery. Therefore, the compressor is a vital component of a BEV motor, ensuring proper functionality of the vehicle. The electric compressor of a BEV considered in this study is shown in Figure 2.1.

Figure 2.1: *Electric compressor of the BEV in this study.*

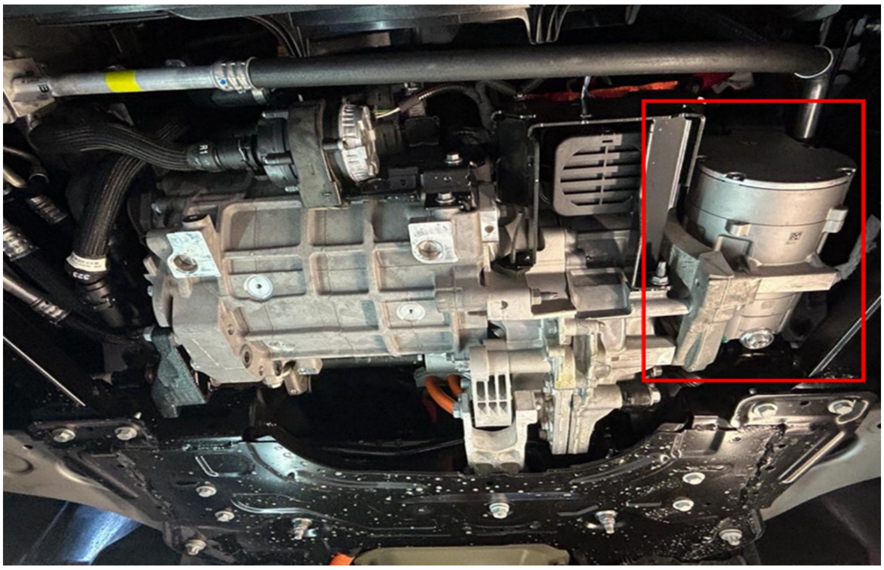

Electric compressors are one of the components that contribute the most to external noise in BEV motors. To quantify the external noise in a BEV vehicle, Exterior noise levels were measured using microphones positioned at the front of the vehicle, 1.65 meters above the ground and 1 meter ahead of the frontmost point of the air grille, while vehicle was idling in a semi-anechoic chamber. Additionally, measurements were made in the vehicle cabin at 22°C with the air conditioning turned on. The HVAC blowers were set to minimum speed during the test, and the A/C was set to 17°C. The details of the hardware and software used in the test are given in Table 2.1.

Table 2.1: *Hardware and software used in vehicle testing.*

Hardware / Software	Description	Model
Microphone	1/2 ” Free Field	ICP
Data Acquisition System	Data Acquisition	LMS
Software	Analysis Software	Siemens Test Lab
Impedance Tube	Material Test	Autoneum

2.2 Test Results on BEV for Compressor Noise Problem

In this section, the compressor noise maneuver tests, based on the detection of problem, for the air borne noise, are explained in detail. The tests are performed in the Semi Anechoic Room as shown Figure 2.2 and climatic chamber as shown in Figure 2.3.

Figure 2.2: *Semi Anechoic Room.*

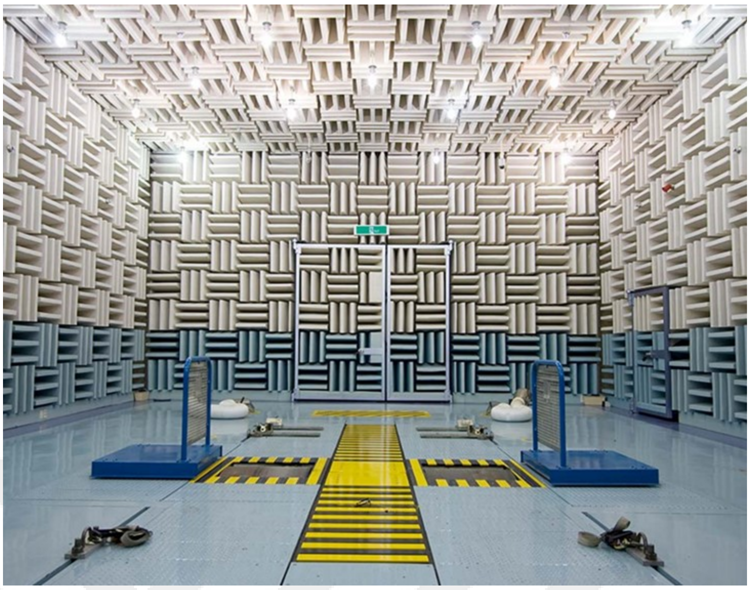

Figure 2.3: *Climatic Chamber.*

For that purpose, A Vehicle is prepared to setup installation that is microphone locations, data gathering system Scadas and setup organization in Siemens Test Lab Program. Overall noise and background noise levels at the vehicle's front microphone were measured as 49.4 dB(A) and 20 dB(A), respectively. The results show a noise problem of 42 dB(A) between 400 and 800 Hz when the A/C is on both ambient and 35°C temperatures. The colormap plots at 22°C is shown in Figure 2.4 Similarly, 3rd octave SPL level results are plotted in Figure 2.5.

Figure 2.4: *Colormap plot at 22°C temperature.*

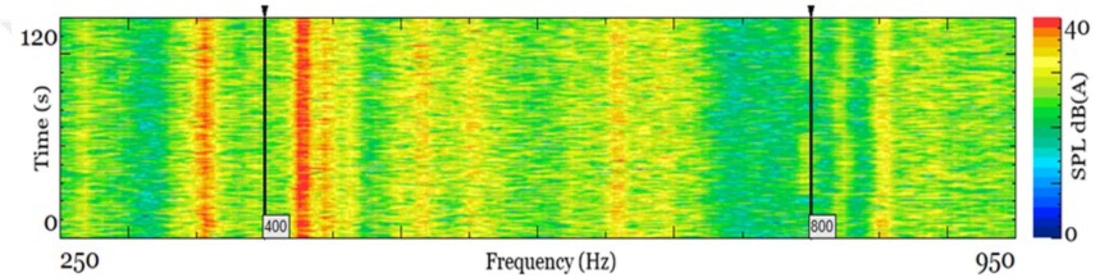

Figure 2.5: *3rd Octave band SPL level measurement at 22°C.*

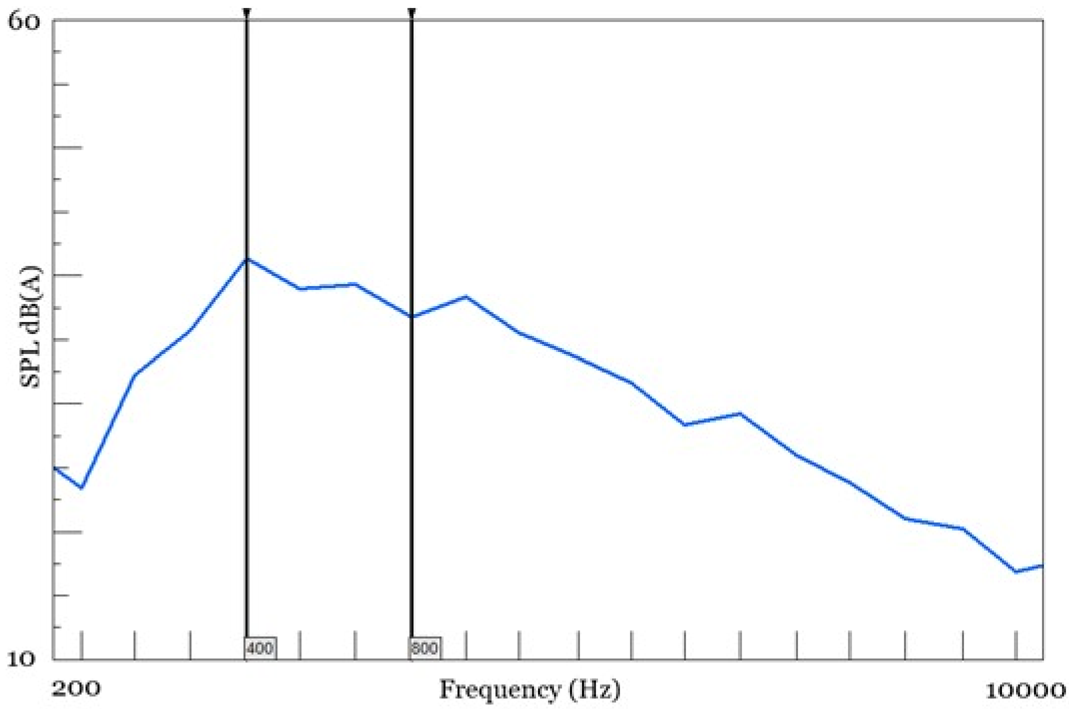

This study aims to design a new sound insulator that will reduce the SPL levels between 400 and 800 Hz by 2 dB(A) to meet customer acceptance. The design framework is presented in the following sections.

3. ANALYSIS METHODS

In this chapter, the analysis methods used in the proposed design and optimization are presented. More specifically, design of metaporous unit cell is detailed in Section 3.1, the details of the theoretical acoustic models are given in Section 3.2. Finally, the simulation method used in the finite element model is explained in Section 3.3.

3.1 Design Methodology

The design methodology consists of Helmholtz Resonator, Aluminum reflection and porous media principles. Figure 3.1 (a) illustrates 3D Design of proposed meta composite porous material and Figure 3.1 (b) shows a perforated cylindrical HR unit cell of proposed meta porous material and the cross section of the unit cell. The incident sound waves are assumed to be normal plane harmonics and the upper surface of the meta porous material is connected to air and receives incident sound waves, and boundaries are connected to porous layers and Helmholtz resonator (HR). Aluminum sides are used for hard rigid walls and porous metamaterials used polyurethane material for Upper Porous Layer is perforated cylindrical gaps to generate HR and Table 3.1. shows parameters of sample (unit mm). Furthermore, Lower Porous Layer increases the absorption of low frequency performance of HR.

Figure 3.1: *(a) Diagrams of the 3D Meta Porous Material. (b) The cross-section of one unit of the Meta Porous in xz plane.*

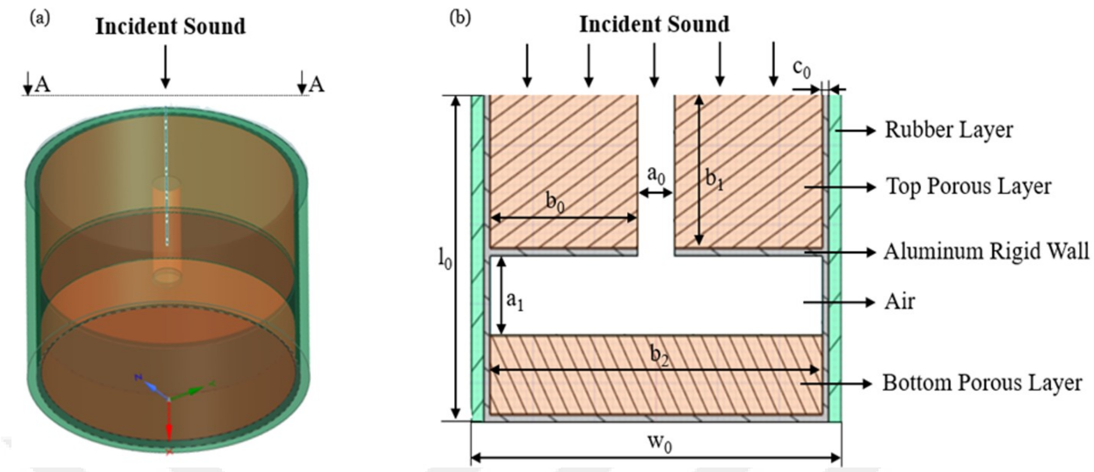

Table 3.1: *The design parameters of the meta porous structure.*

Parameters of Sample	Dimensions (mm)
a_0	6
a_1	10
b_0	27
b_1	18
b_2	54
c_0	1
l_0	40
w_0	60

3.2 Theoretical Method

In this section some of the theoretical to models are summarized to model poroacustic behavior of the materials.

3.2.1 Delany-Bazley-Miki Acoustic Model

The Delany-Bazley model is an approach used to predict the acoustic properties of porous materials, particularly their sound absorption and impedance characteristics. It is based on the knowing the static air flow resistivity of the material, acoustic impedance and sound absorption coefficient can be estimated [41, 42, 43, 44]. The characteristic impedance of the porous material is given by:

$$\frac{Z_c}{c_0\rho_0} = 1 + 0.0571\left(\frac{f}{\sigma}\right)^{-0.754} - j \cdot 0.087\left(\frac{f}{\sigma}\right)^{-0.732} \tag{3.1}$$

where Z_c is the complex characteristic impedance, ρ_0 is the air density, c_0 is the speed of sound, f is the frequency of the sound wave, and σ is the flow resistivity of the material.The complex wave number is given by:

$$\frac{k}{\frac{w}{c_0}} = 1 + 0.0978\left(\frac{f}{\sigma}\right)^{-0.700} - j \cdot 0.189\left(\frac{f}{\sigma}\right)^{-0.595} \tag{3.2}$$

where k is the complex wave number and ω is the angular frequency.

3.2.2 BIOT-Allard Acoustic Model for Porous Media

The Biot-Allard model is an advanced theoretical framework used to describe the acoustic behavior of porous materials, accounting for both the solid and fluid phases within the material [45, 46, 47]. This model is an extension of the Biot theory of poroelasticity, which provides a detailed description of wave propagation in fluid-saturated porous media. The Biot-Allard model is particularly useful for predicting sound absorption and transmission in materials where the interaction between the solid matrix and the fluid phase plays a significant role. The model predicts the existence of two types of compressional waves (fast and slow) and one shear wave, with their corresponding wave numbers:

$$k_{\text{fast}} = \frac{\omega}{c_{\text{fast}}}, \quad k_{\text{slow}} = \frac{\omega}{c_{\text{slow}}}, \quad k_{\text{shear}} = \frac{\omega}{c_{\text{shear}}} \tag{3.3}$$

where c_{fast}, c_{slow}, and c_{shear} are the phase velocities of the fast compressional wave, slow compressional wave, and shear wave, respectively. The surface impedance (Z) and absorption coefficient (α) can be calculated from the wave numbers and material properties:

$$Z = \frac{1}{\sqrt{\rho_{\text{eq}} K_{\text{eq}}}} \left(\frac{k_{\text{fast}} + k_{\text{slow}}}{k_{\text{fast}} - k_{\text{slow}}} \right) \tag{3.4}$$

and

$$\alpha = 1 - \left| \frac{z - z_0}{z + z_0} \right|^2 \tag{3.5}$$

where ρ_{eq} and K_{eq} are the effective density and bulk modulus of the porous material, and Z_0 is the characteristic impedance of air.

3.2.3 Wilson's Acoustic Model

Wilson's model is a semi-empirical approach to predicting the acoustic properties of porous materials[48]. Developed by David K. Wilson, this model is particularly useful for materials like ground surfaces or fibrous media, where the geometric complexity of the pores and the interaction of sound waves with the material require more detailed modeling than simpler empirical models can provide and thermal and viscous effects that occur in porous media have the characteristic of a relaxation process [49, 50, 51]. The characteristic impedance is given by:

$$\frac{Z_c}{\rho_0 c_0} = \frac{1}{\varphi} \left(1 + \frac{\gamma - 1}{1 + j\frac{\varphi\omega}{\sigma}} \right)^{1/2} \left(1 + j\frac{\varphi \rho_0 \omega}{\sigma} \right)^{1/2} \tag{3.6}$$

where Z_c is the complex characteristic impedance, ρ_0 is the density of air, c_0 is the speed of sound, ϕ is the porosity, σ is the flow resistivity, ω is the angular frequency, and γ is the ratio of specific heats. Surface impedance is given by:

$$Z_s = Z_c \coth(jkd) \tag{3.7}$$

where Z_s, k, and d are the surface impedance, wave number, and thickness of the porous layer, respectively, and the sound absorption coefficient α is given by:

$$\alpha = 1 - \left| \frac{Z_s - Z_0}{Z_s + Z_0} \right|^2 \tag{3.8}$$

3.2.4 Equivalent Fluid Density Acoustic Model

The Equivalent Fluid Density Model (EFDM) is a simplified theoretical approach used to predict the acoustic behavior of porous materials [52, 53]. The model is based on the concept of treating the porous medium as an equivalent homogeneous fluid with modified properties, namely an equivalent density and bulk modulus [54]. This model is particularly useful in scenarios where the structure of the solid frame does not contribute significantly to the wave propagation, allowing for a simpler analysis compared to more complex models like Biot's theory [55]. The equivalent density accounts for the additional inertia imposed by the porous structure on the fluid motion. It is typically expressed as:

$$\rho_{\text{eq}} = \frac{\rho_0 \varphi}{\varphi + (1 - \varphi) \wedge} \tag{3.9}$$

where ρ_0 is the density, ϕ is the porosity, and Λ is the correction factor related to tortuosity. The equivalent bulk modulus, which represents the compressibility of the medium, is given by:

$$K_{\text{eq}} = \frac{K_0}{\varphi + \frac{(1-\varphi)}{\wedge x}} \tag{3.10}$$

where K_0 is the bulk modulus of the fluid in the pores, and x is a correction factor related to the thermal exchanges between the fluid and the solid matrix. The complex wave number is given by:

$$k = \omega\sqrt{\frac{\rho_{\text{eq}}}{K_{\text{eq}}}} \tag{3.11}$$

Where ω is the angular frequency. The characteristic impedance of the equivalent fluid is defined as:

$$Z_c = \sqrt{\rho_{\text{eq}} K_{\text{eq}}} \tag{3.12}$$

The surface impedance Z_s of the porous material, considering the thickness d, can be calculated as:

$$Z_s = Z_c \coth(jkd) \tag{3.13}$$

And the sound absorption coefficient α is given by:

$$\alpha = 1 - \left|\frac{Z_s - Z_0}{Z_s + Z_0}\right|^2 \tag{3.14}$$

where Z_0 is the characteristic impedance of air.

3.2.5 Johnson–Champoux–Allard (JCA) Acoustic model

In this section, based on the Johnson–Champoux–Allard (JCA) model [56, 57, 58, 59], the air-saturated porous material can be considered as a homogeneous effective fluid. The effective density ρ_{eff} and bulk modulus K_{eff} can be described as:

$$\rho_{\text{eff}} = \frac{\rho_0 \alpha_\infty}{\phi}\left(1 + \frac{i\omega_v}{\omega}\sqrt{1 - i\eta\rho_0\left(\frac{2\alpha_\infty}{\sigma\phi\lambda}\right)^2}\right) \tag{3.15}$$

and

$$K_{\text{eff}} = \frac{\gamma P_0}{\phi \left(\gamma - (\gamma - 1) \left[1 + \frac{i\omega_c'}{P_r\omega} \frac{\rho_0 \alpha_\infty}{\phi} \sqrt{1 - i\eta\rho_0\omega \left(\frac{2\alpha_\infty}{\sigma'\phi\lambda'} \right)^2} \right]^{-1} \right)} \tag{3.16}$$

where ρ_0 is the air density, P_0 is the atmospheric pressure, η is the air dynamic viscosity, γ is the specific heat ratio, and Pr is the Prandtl number. Furthermore, the angular Biot number ω_v can be explained as:

$$\omega_v = \frac{\sigma\phi}{\rho_0 \alpha_\infty} \tag{3.17}$$

and adiabatic cross-over angular frequencies can be described as:

$$\omega_c' = \frac{\sigma'\phi}{\rho_0 \alpha_\infty} \tag{3.18}$$

Other parameters that describe the acoustic properties of porous material are porosity ϕ, tortuosity α_∞, flow resistivity σ, thermal characteristic length λ', viscous characteristic length λ, and thermal resistivity, which are given:

$$\sigma' = \frac{8\alpha_\infty \eta}{\phi\lambda'} \tag{3.19}$$

The complex wave number k in the porous medium is defined as:

$$k(\omega) = \omega \sqrt{\frac{\rho_{\text{eff}}(\omega)}{K_{\text{eff}}(\omega)}} \tag{3.20}$$

The characteristic impedance of the medium is given by:

$$Z_c(\omega) = \sqrt{\rho_{\text{eff}}(\omega)\, K_{\text{eff}}(\omega)} \tag{3.21}$$

This impedance is used to calculate the reflection and transmission of sound waves at interfaces involving the porous material. The surface impedance Z_s of the material can be calculated using the characteristic impedance and the wave number:

$$Z_s(\omega) = Z_c(\omega) \coth(jk(\omega)d) \tag{3.22}$$

where d is the thickness of the porous layer. The sound absorption coefficient $\alpha(\omega)$ is given by:

$$\alpha(\omega) = 1 - \left| \frac{Z_s(\omega) - Z_0}{Z_s(\omega) + Z_0} \right|^2 \tag{3.23}$$

where Z_0 is the characteristic impedance of air.

3.3 Simulation Model

A frequency domain simulation of COMSOL Multiphysics software selected for the interfaces in the Poroacoustics Module that are based on the finite element method (FEM). Figure 3.2 shows the geometry of the 3D modeled system. The plane wave used in the upper port with incident angle q=0° is modeled as a background pressure field with an amplitude of 1.0 Pa. The rigid boundary condition are applied to the walls. Aluminum walls determined as reflective walls. Upper and lower Polyurethane Foam are modeled as porous layer and the boundaries determined as sound hard wall boundary. Surrounded rubber layer designed as rubber and used as connecting piece of model system.

Figure 3.2: *Comsol Frequency Domain 2D and 3D Model.*

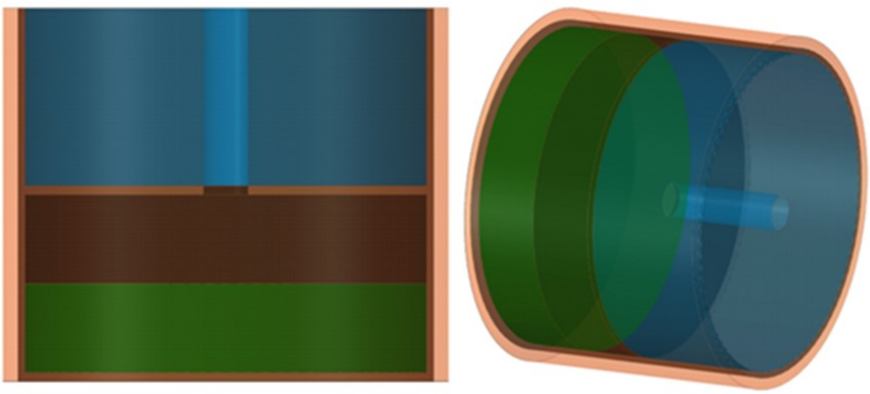

Absolute pressure is performed as input, and the surrounding medium is air with density $\rho_0 = 1.21\,\text{kg/m}^3$ and sound speed $c_0 = 343\,\text{m/s}$. The walls are modeled as being acoustically rigid with respect to air due to the huge impedance mismatch between them. The porous matrix approximation selected the limp model because of the polyurethane structure. The porous material is described by the Johnson Champoux-Allard (JCA) model in the poroacoustics domain, and the physical properties of the porous material of the developed 3D model in terms of the JCA model are shown in Table 3.2.

Table 3.2: *Physical Properties of the Porous Material*

Air Flow Resistivity	Open Porosity	Tortuosity	Viscous Length	Thermal Length	Density	Thickness
σ [Ns/m^4]	ϕ [–]	α_∞ [–]	Λ [μm]	Λ' [μm]	ρ [kg/m^3]	mm
5458	0.9	1.03	83	267	50	40

The modelling used frequency-based mesh in Comsol selected extremely fine mesh criteria. The maximum mesh element size frequency was determined as 3150 Hz. The tetrahedral element was determined as the mesh element type and a mesh with 538154 elements performed on model. Furthermore, Mesh quality was evaluated based on skewness and growth rate. The average skewness and growth rate are 0.7113 and 0.6496 respectively. In this study, the suggested model results are shown in Figure 3.3 for specified frequencies.

Figure 3.3: *(a) 400Hz (b) 500Hz (c) 600Hz (d) 700Hz Acoustic sound pressure level results on suggested design.*

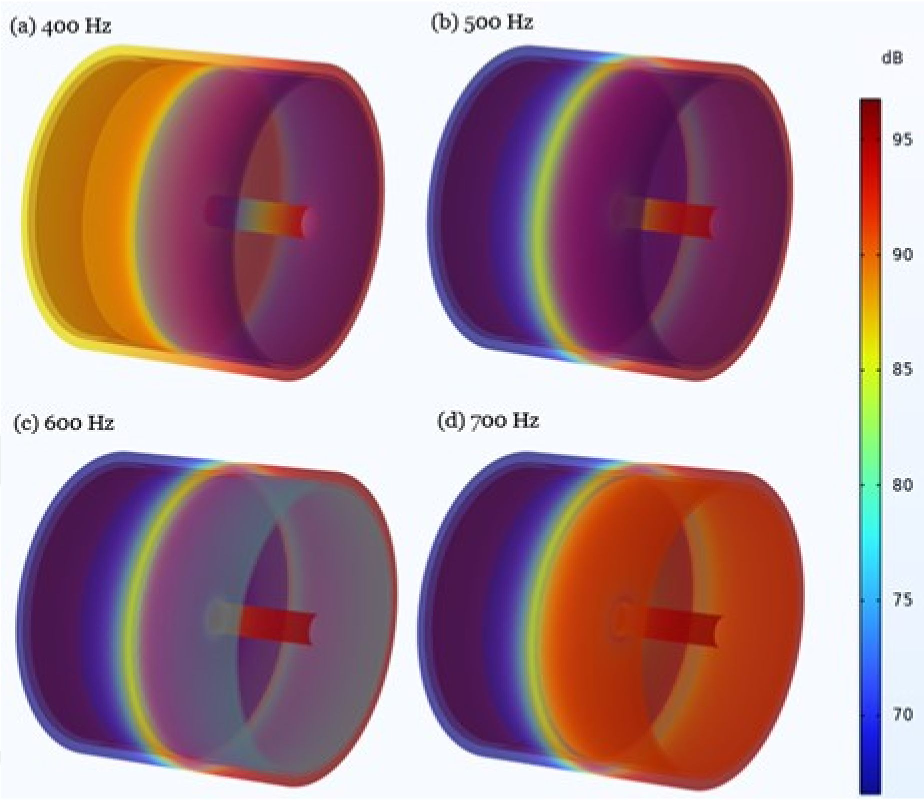

Simulation results show that sound absorption becomes effective starting at 350 Hz and reaches maximum values between 500 and 600 Hz, thanks to the Helmholtz resonator effect. The air cavity, combined with aluminum and porous material, enhances broadband low-frequency acoustic absorption. Furthermore, the polyurethane placed at the bottom proves effective in the low-frequency absorption performance. Impedance tube measures the acoustic performance of the sound package.

4. OPTIMIZATION METHODOLOGY

In this chapter, design parameter examined as a way of Taguchi method with details of optimization strategy in Section 4.1.

4.1 Taguchi Experiment Design Parameters of ANOVA Method

One of the main objectives of this thesis is to evaluate and benchmark the accuracy and computational performance of the proposed method in comparison to four recent optimization designs, the optimization parameters are determined using a systematic approach. This section presents a detailed application of the Taguchi method for tuning the parameters of the proposed optimization in composite design. This revision enhances clarity and flow while Mean values consisting of absorption coefficient are used to determine the best levels of the design factors by reducing the variance for the design of Anova parameters in the Taguchi method [60, 61, 62, 63]. The underlying principle of this method is to show the variance of the mean value (absorption coefficient), which is considered as the objective function. Thus, This method allows us to gain insights into the impact of multiple design factors while minimizing the number of experiments required. The brief description of the five main steps is as follows:

Plan: The objective, measurement method, and possible noise attenuation techniques are defined in this step.

Design: The noise affection factors, simulation techniques, boundary conditions, material properties, and objective functions are designed according to the theoretical information and literature experiments in this step.

Conducting: The simulations and existing methods are verified and combined with a new design parameters approach, and simulations are conducted based on the information from Phase 2 and verified simulations.

Analysis: The results from the previous step are analyzed to determine the best design model using the one-way ANOVA method. Various techniques, such as the mean value method, are performed to analyze the results based on the simulation conditions.

Verification: One of the best results from Phase 4 analysis is verified by conducting experimental tests in the impedance tube. Additionally, the expected improvement on the vehicle is verified with the new metamaterial design concept, focusing on the vehicle compressor noise transfer path in the final step.

One-Way ANOVA – Taguchi method is a statistical method used when we're looking at the impact of one single factor on design factors [64]. For that purpose, the design factors are analyzed one by one and the effect of one design factor is estimated on absorption coefficient in this study. The experimental process is designed with Taguchi's Main Effect Plot to reduce the prototype numbers and to find optimum design. These optimal design parameters are identified with the Anova Main Effect Plot method between 400 and 800 Hz and determined the most effective parameter on absorption coefficient with Anova Main Effect Plot in Minitab 20. The selection of design depends on mean value (absorption coefficient) to be studied. Design Configuration are shown on Table 4.1.

Table 4.1: *Design configuration of effected parameters on developed design*

Design Configs	Neck Diameter t_i, mm	Air Internal Height s_i, mm	Bottom Polyurethane Height y_i, mm
Config 1	2	10	10
Config 2	3	10	10
Config 3	4	10	10
Config 4	5	10	10
Config 5	6	10	10
Config 6	7	10	10
Config 7	8	10	10
Config 8	9	10	10
Config 9	10	10	10
Config 10	6	5	10
Config 11	6	15	10
Config 12	6	10	0

Neck Gap Effect (t_i), Air Internal Thickness (s_i) and Lower Polyurethane Thickness (y_i) are examined with Simulation Analysis on design configuration shown details in Figure 4.1.

Figure 4.1: *Investigated parameters on design solution.*

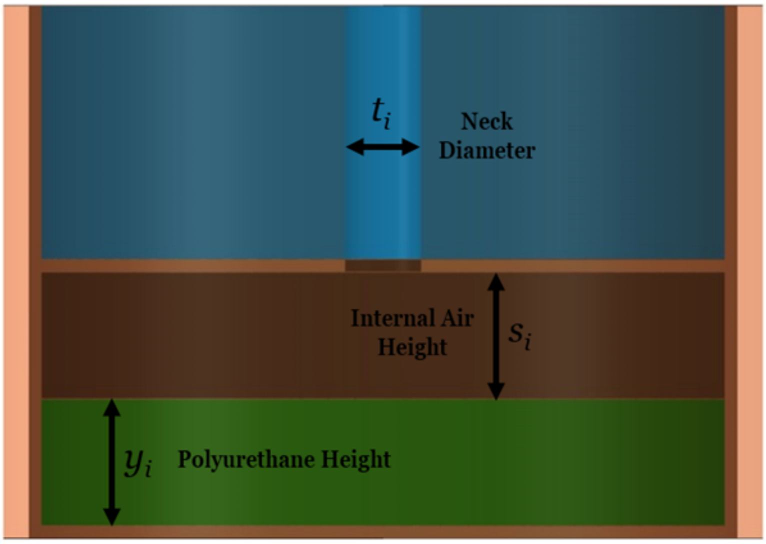

The Taguchi Anova method performs a one way factor analysis to select a suitable computational method for each parameter. The results of the one factor Anova method study are shown in Figure 4.2. The effect of neck gap on the absorption coefficient is shown in Figure 4.2 (a). Design configuration-5 showed the best performance in terms of Helmholtz neck gap and rigid aluminum cavity related to desired frequencies. Similarly, the effect of the internal thickness is shown in Figure 4.2 (b). The results indicate that configuration-5 is the best design, whereas configuration-10 reduces the low frequency performance. Finally, the effect of the height of the polyurethane placed at the bottom is shown in Figure 4.2 (c). The results indicate that configuration-5 delivers the best performance in terms of the absorption coefficient within the frequency range of 400 Hz to 800 Hz. In contrast, configuration-12 exhibits the poorest performance on the absorption coefficient.

Figure 4.2: *Main effect results on average absorption coefficient between 400 and 800 Hz; (a) neck gap, (b) air interval, (c) bottom porous.*

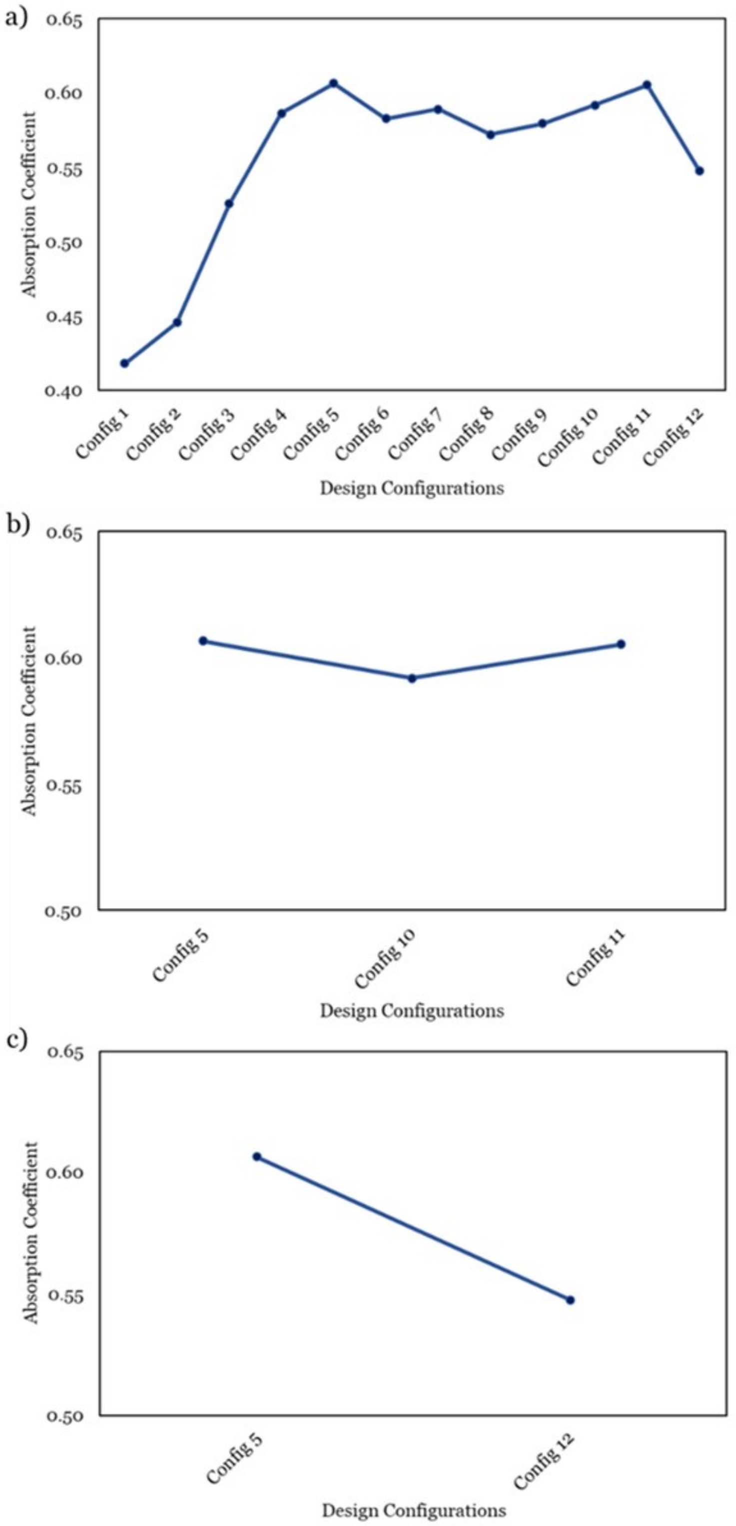

5. RESULTS AND DISCUSSION

In this section, first the COMSOL Polyurethane (PU) model is validated against the experimental result with using the polyurethane foam compared with impedance tube measurement. Subsequently, both proposed design results are compared with impedance tube measurements and validated in detail in Section 5.1 and Vehicle level test results are shown in Section 5.2. Furthermore, Summary is given in Section 5.3.

5.1 Impedance Tube Validation of the PU Foam and proposed design configuration

Impedance tube measures the acoustic performance of the sound-package. The microphones measure the sound pressure levels at both ends of the tube. By comparing the input and output signals, the absorption coefficient of the material is determined using LabVIEW software. The experimental set-up is shown in Figure 5.1.

Figure 5.1: *Impedance tube measurement.*

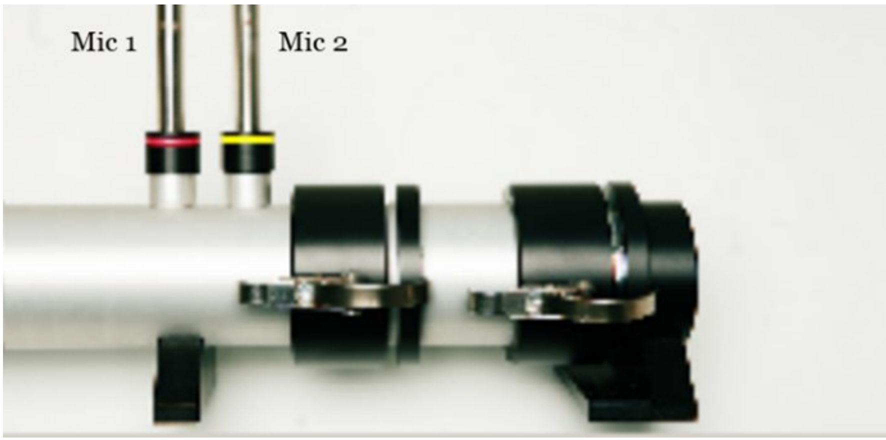

We validated the COMSOL model against the experimental test of polyurethane foam with a thickness of 40 mm to ensure the simulation methodology. The parameters of the model such as material properties, boundary conditions, and empirical formulas are defined similarly to those found in the literature [65, 66, 67]. Harmonic acoustic analyses were conducted in the frequency domain, and the sound propagation was determined numerically. The COMSOL results are compared with the experimental test results in impedance tube in Figure 5.2. The results show a high correlation between the test results and the COMSOL model. More specifically, the relative error on the maximum absorption coefficient is 6%, and the root mean square (RMS) error is only 4.54%. The COMSOL model is validated using impedance tube measurements.

Figure 5.2: *Polyurethane foam comparison of test results vs COMSOL Simulation.*

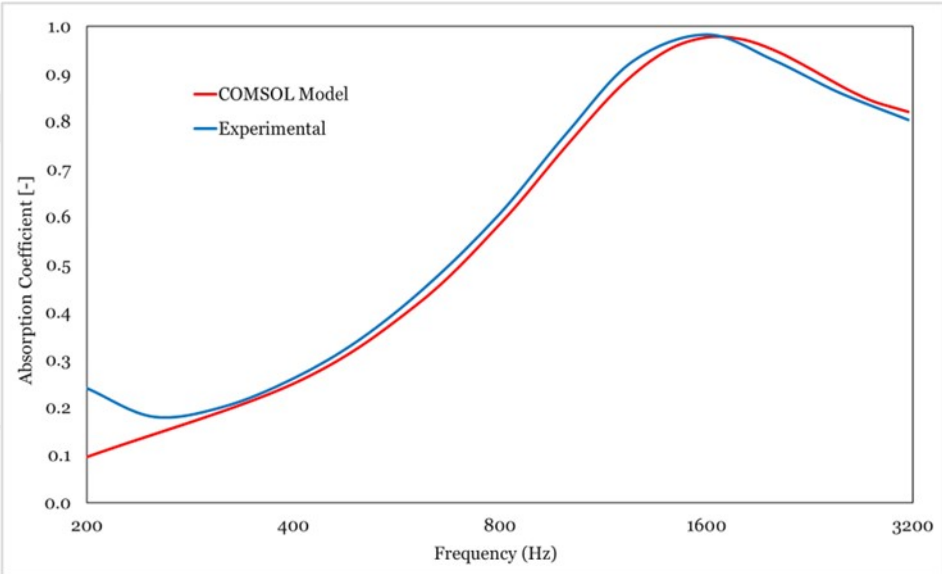

The COMSOL model of proposed design configuration is validated using impedance tube measurement. After polyurethane foam absorption is validated with both impedance tube experiment and COMSOL model, metaporous structure (proposed as configuration 5) is produced and tested in impedance tube to determine absorption coefficient. The comparison between impedance tube test and COMSOL simulation output is shown in Figure 5.3.

Figure 5.3: *Simulation and Experimental Test Results of configuration 5.*

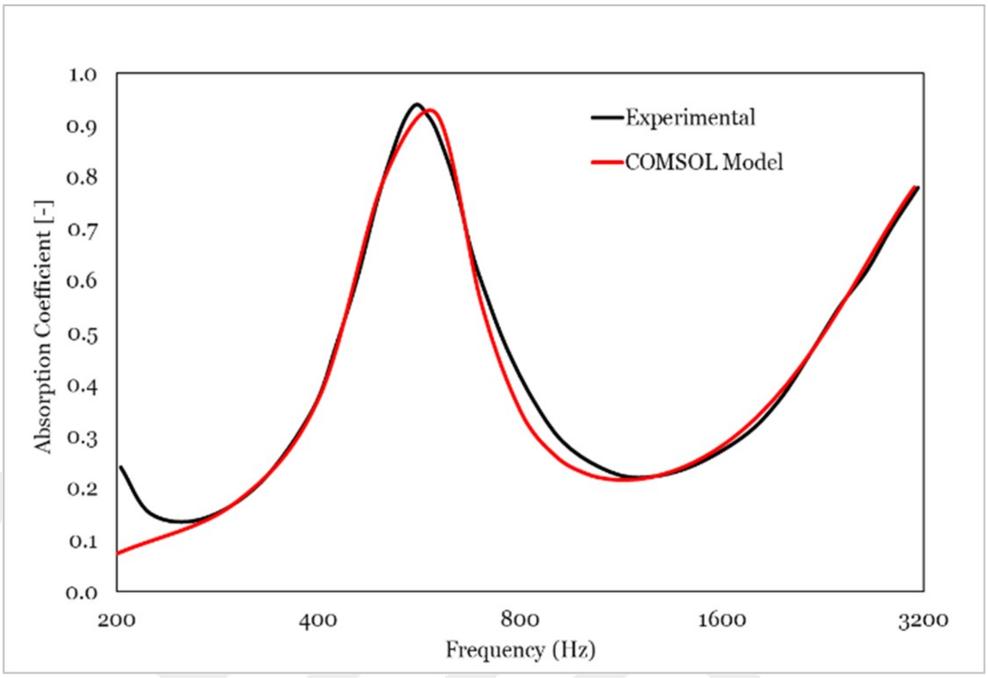

This test is conducted under conditions of 22 °C and 52% air humidity. Figure 5.3 exhibits that our COMSOL methodology captures the 400-800 absorption of the selected meta-porous topology and this result was verified with later impedance tube experiments. The general agreement between the experiment and the simulation model is commendable above 300 Hz. The lower frequency mismatch can be attributed to the difficulty of low-frequency detection with standard impedance tube experiments.

5.2 Vehicle Tests

Vehicle-level tests assess the overall acoustic and vibrational performance of a vehicle to ensure comfort, and compliance with regulations in NVH. These tests evaluate how noise, vibrations, and harshness levels are transmitted to the occupants and the environment under various driving conditions. Specifically, in electric vehicles, compressor noise becomes more prominent due to the absence of motor noise and accessories.

The cooling systems use electric compressors, which can generate high-pitched sounds or tonal noise both vehicle cabin side and environment. Due to mechanical vibration transmission and pulsation in refrigerant flow, low frequency problem was shown in motor idling maneuver. The vehicle tests in the NVH acoustic chamber consist of the following stages:

- Test Planning
- Sensor and equipment selection (e.g., microphones, accelerometers)
- Vehicle Check (e.g., tire pressure, components)
- Software Setup Installation
- Sensor Calibration
- Test Execution
- Post Processing

The proposed resonator design was tested on a vehicle to evaluate its functionality. For this purpose, the resonators were installed within the empty box designed for the compressor. This box is fully enclosed to minimize noise sources, particularly on the bottom side. The vehicle level tests were carried out in 3 stages: 1) vehicle without any resonator, 2) vehicle with an empty box, containing the resonators, and 3) vehicle equipped with resonators placed in a box suitable for vehicle installation. The resonators in the empty box are shown in Figure 5.4 (a), while Figure 5.4 (b) depicts the vehicle with the installed box.

Figure 5.4: *The proposed resonator design (a) placed in a box for vehicle assembly, (b) vehicle installation.*

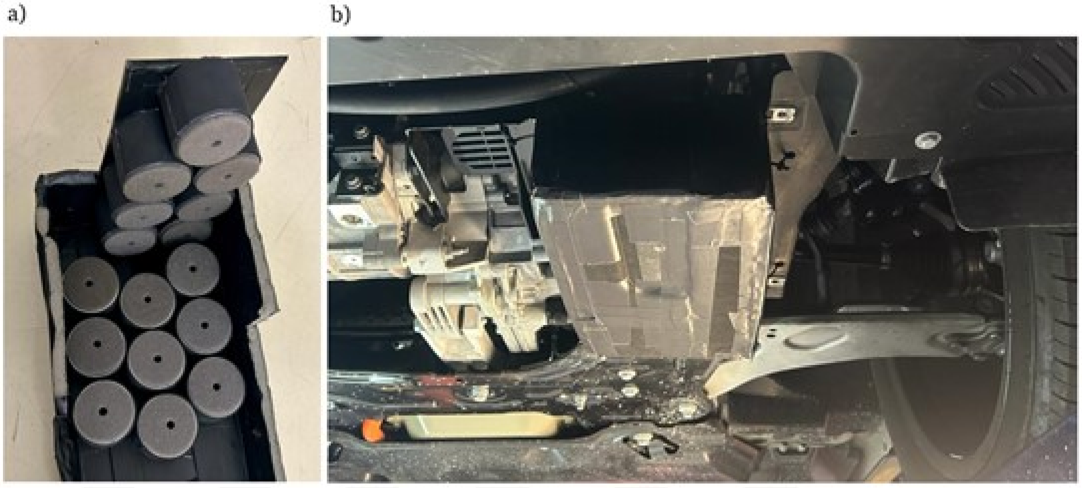

The colormap comparisons of the base vehicle and base vehicle with empty box are shown in Figure 5.5 (a) and Figure 5.5 (b) respectively. Finally, the results for the resonator design installed in the base vehicle are shown in Figure 5.5 (c). In addition, the 3rd octave measurement results are given in Figure 5.6.

Figure 5.5: *Comparison of the test results (a) Base vehicle, (b) Base vehicle including the empty box, and (c) Base vehicle with the proposed resonator design.*

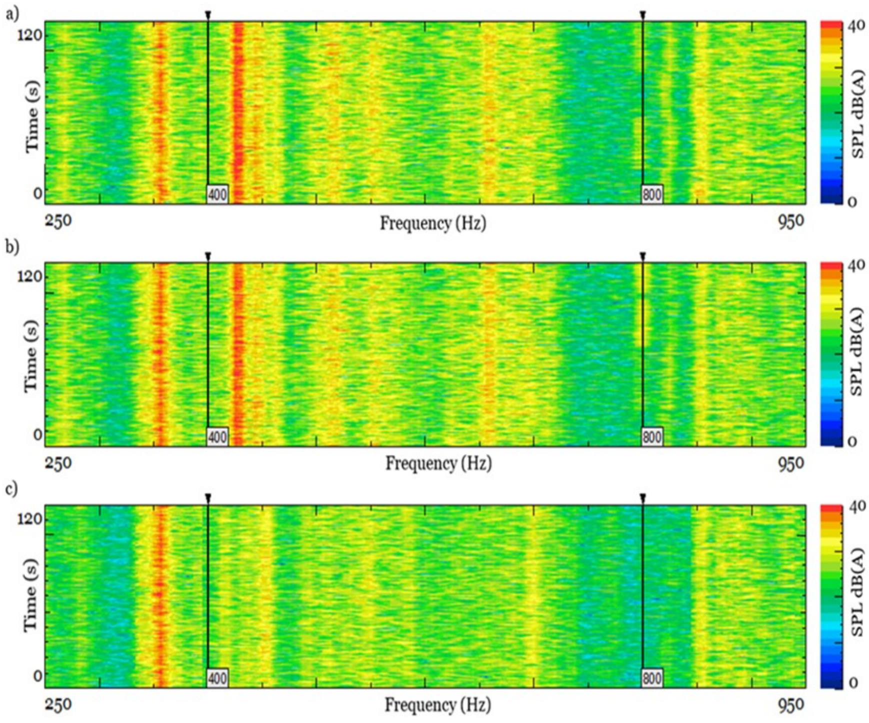

Figure 5.6: *3rd octave band SPL level measurement at 22°C.*

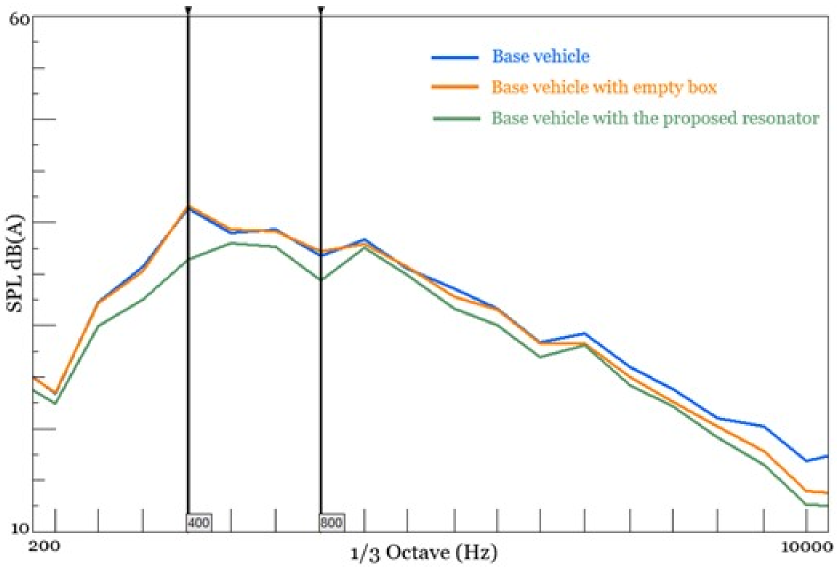

Virtual colormap simulations were performed to visualize noise, vibration, and harshness data and analyze the primary contributors to the external noise performance of the vehicle. The results were post-processed with 3.125 Hz frequency resolution, and 3rd octave curves were used to understand the noise and vibration characteristics in the specified frequency range. The blue and orange curves represent the base vehicle and base vehicle with empty box measurements, respectively, while the green curves symbolize the base vehicle with the proposed meta-porous materials design. The results show that proposed metaporous design is effective between 400 and 800 Hz, providing 62% absorption. Furthermore, our design parameters are effective in increasing broadband performance for such a design concept. In terms of electric vehicle test of norms, idle mode tests are conducted in a semi-anechoic chamber with the A/C on, and the room temperature maintained at 22 °C. During these tests, the proposed resonator design provided an improvement of approximately 3 dB(A) in the overall noise level for the exterior microphone. Furthermore, this proposed design can be extended to other applications and used for addressing low frequency problems in vehicles, such as road noise.

5.3 Summary

A new metaporous composite material prototype design was proposed to solve airborne radiated compressor noise problem based on vehicle application and verification in terms of experimental results. This framework is validated by comparing the simulation model and the measured absorption coefficient in terms of impedance tube. With the help of this framework validation, vehicle level tests are conducted as metamaterial application covering e-compressor on vehicle. The parameters of design framework can stand out by one way ANOVA method between main methods of geometry and main value of absorption coefficient. The proposed hybrid composite design combines this effected parameter to identify frequency band width and absorption performance. To find a more reliable simulation results for these parameters, Simulation of porous JCA model is validated from the literature in terms of 5 important material properties. From this perspective, simulation results are conducted as the reference of design parameters step by step. The best results of these parameters combination show that proposed meta porous design is effective between 400 and 800 Hz., providing 62% absorption. Moreover, this study shows that the proposed design can identify an improvement of more than 3 dB(A) in exterior noise of vehicle. The design framework proposed is expected to pave the way for improved noise reduction performance for new generation electric vehicles. The research findings indicate that the new hybrid method has great potential to improve alternative material application in vehicle for engineering problems efficient.

6. CONCLUSIONS

In this thesis, air-borne radiated compressor noise problem was investigated on electric vehicle and a new prototype design is developed with a particular focus on low-frequency for this exterior noise problems. This research introduced a meta-porous topology model that effectively integrates a Helmholtz resonator with aluminum and porous materials. In the design phase, with using the Taguchi design method, key parameters were optimized to enhance the model's performance, allowing a tailored response to low-mid frequency noise. Furthermore, Simulations provided insights into the physical properties of the porous layers, surface impedance, and cavity effects, and were validated through impedance tube measurements. Results demonstrated that the proposed design achieves around 60% noise reduction effectiveness in the targeted frequency range, proving the potential of meta-porous materials to mitigate airborne compressor noise in electric vehicles and meaningful real-world implications. Furthermore, this study, as electric vehicles become more prevalent, addresses noise concerns not only enhances user comfort but also contributes to reducing noise pollution in urban environments. Moreover, this model offers an adaptable framework that could be integrated into various vehicle platforms, providing manufacturers with an effective approach to tackle low-frequency noise issues inherent to electric propulsion systems. By improving the soundscape of electric vehicles, this work supports the goal of creating quieter, more environmentally friendly transportation options, which can enhance quality of life in densely populated areas. In terms of future research, exploring alternative materials and structures for the meta-porous design may yield even greater noise reduction performance, especially in varied frequency ranges. Additionally, adapting this model for integration with other vehicle components, such as panels or enclosures, could allow for broader application across different noise sources within the vehicle. Subsequent vehicle-level tests in a semi-anechoic environment under controlled conditions confirmed an exterior noise reduction exceeding 3.1

dB(A). This outcome highlights the design's viability and presents a promising approach for new-generation electric vehicles, aligning with industry goals for quieter, more sustainable transport solutions. Future research could extend this framework to varying noise profiles and expand material exploration for enhanced adaptability across electric vehicle platforms.

7. FUTURE WORKS

NVH insulation performance of proposed metaporous composite design is improved with different optimization approaches in this thesis. Although, it is accomplished by the validation of design schemes, there can be further improvements can be achievement by different approaches. These can be summarized as:

- By changing the materials on the proposed design and examining these materials as design parameters, investigating their effect using the Taguchi method.
- Creating databases by modifying the dimensions of the proposed design parameters and adjusting them according to higher frequencies and the corresponding problems.
- Arranging the proposed resonator in the form of a flat sample suitable for the Alpha cabin and evaluating the absorption coefficient in a diffuse field.
- By developing a resonator form for other air borne noise issues in the 400-800 Hz range on the vehicle and placing this form in the noise transfer paths, evaluating its effect.
- To increase broadband and find design parameters for lower frequencies (<400 Hz), these parameters can be combined with the proposed design parameters to create a new hybrid design.

REFERENCES

[1] S. Nayak and D. Chatterjee, "Nvh product development process in the indian automotive industry," tech. rep., SAE Technical Paper, 2013.

[2] F. Cavaliere, S. Zlotnik, R. Sevilla, X. Larrayoz, and P. Díez, "Nonintrusive parametric nvh study of a vehicle body structure," *Mechanics based design of structures and machines*, vol. 51, pp. 6557–6582, Aug. 2023.

[3] H. Xue, G. Previati, M. Gobbi, G. Mastinu, *et al.*, "Research and development on noise, vibration, and harshness of road vehicles using driving simulators-a review," *SAE INTERNATIONAL JOURNAL OF VEHICLE NOISE AND VIBRATION*, vol. 7, pp. 555–577, Apr. 2023.

[4] L. Sangiuliano, B. Reff, J. Palandri, F. Wolf-Monheim, B. Pluymers, E. Deckers, W. Desmet, and C. Claeys, "Low frequency tyre noise mitigation in a vehicle using metal 3d printed resonant metamaterials," *Mechanical Systems and Signal Processing*, vol. 179, p. 109335, Nov. 2022.

[5] D. He, D. Ziviani, and Y. Liu, "Theoretical analysis of noise and vibration generated by gas pressure pulsation in hermetic compressors," *International Compressor Engineering Conference*, 2021.

[6] H. Xue, G. Previati, M. Gobbi, G. Mastinu, *et al.*, "Research and development on noise, vibration, and harshness of road vehicles using driving simulators-a review," *SAE INTERNATIONAL JOURNAL OF VEHICLE NOISE AND VIBRATION*, vol. 7, pp. 555–577, Apr. 2023.

[7] Z. Mao, M. Feng, and Y. Lin, "Application of sound package material in noise reduction of motor," *Vibroengineering Procedia*, vol. 36, pp. 66–71, 2021.

[8] Z. Mao, M. Feng, and Y. Lin, “Application of sound package material in noise reduction of motor,” *Vibroengineering Procedia*, vol. 36, pp. 66–71, 2021.

[9] H. Wu, Y. Shen, M. Liang, J. Liu, J. Wu, and Z. Li, “Performance research and optimization of sound insulation hood of air compressor unit,” *Applied Sciences*, vol. 11, no. 21, p. 10364, 2021.

[10] R. Guo, C. Cao, Y. Mi, and Y. Huang, “Experimental investigation of the noise, vibration and harshness performances of a range-extended electric vehicle,” *Proceedings of the Institution of Mechanical Engineers, Part D: Journal of Automobile Engineering*, vol. 230, no. 5, pp. 650–663, 2016.

[11] S.-G. Park, J.-T. Park, K.-W. Seo, and G.-B. Lee, “Comparison of the sound quality characteristics for the outdoor unit according to the compressor model.,” *International Compressor Engineering Conference*, 2012.

[12] G. Leventhall, “Low frequency noise. what we know, what we do not know, and what we would like to know,” *Journal of Low Frequency Noise, Vibration and Active Control*, vol. 28, no. 2, pp. 79–104, 2009.

[13] H. Lee, B.-H. Kwon, and S.-O. Park, “The reduction of the low-frequency band noise in hermetic refrigerator compressor,” *International Compressor Engineering Conference*, 1998.

[14] W. Yu, “Analysis and optimization of low-speed road noise in electric vehicles,” *Wireless Communications and Mobile Computing*, vol. 2021, no. 1, p. 5537704, 2021.

[15] K. Govindswamy and G. Eisele, “Sound character of electric vehicles,” tech. rep., SAE Technical Paper, 2011.

[16] N. Indrianti, N. B. Biru, and T. Wibawa, “The development of compressor noise barrier in the assembly area (case study of pt jawa furni lestari),” *Procedia CIRP*, vol. 40, pp. 705–710, 2016.

[17] Z. Maekawa, J. Rindel, and P. Lord, *Environmental and architectural acoustics*. CRC Press, 2010.

[18] S. Marshall, “Reducing compressor noise while considering system interactions,” *International Compressor Engineering Conference*, 2002.

[19] F. Langfeldt, A. Khatokar, and W. Gleine, “Plate-type acoustic metamaterials with integrated helmholtz resonators,” *Applied Acoustics*, vol. 199, p. 109019, 2022.

[20] J. Mason and F. Fahy, “The use of acoustically tuned resonators to improve the sound transmission loss of double-panel partitions,” *Journal of Sound and Vibration*, vol. 124, no. 2, pp. 367–379, 1988.

[21] S. A. Cummer, J. Christensen, and A. Alù, “Controlling sound with acoustic metamaterials,” *Nature Reviews Materials*, vol. 1, no. 3, pp. 1–13, 2016.

[22] S. Tretyakov, A. Urbas, and N. Zheludev, “Special issue on the history of metamaterials,” *J. Opt.*, vol. 19, p. 080404, 2017.

[23] Z. Zhang, X. Wang, Z. Y. Liu, Q. Fan, and T. R. Lin, “A study of low frequency sound insulation mechanism of a perforated plate-type acoustic metamaterial,” *Journal of Sound and Vibration*, vol. 558, p. 117775, 2023.

[24] J.-L. Auriault, C. Boutin, and C. Geindreau, *Homogenization of coupled phenomena in heterogenous media*, vol. 149. John Wiley & Sons, 2010.

[25] G. Pavan and S. Singh, “Near-perfect sound absorptions in low-frequencies by varying compositions of porous labyrinthine acoustic metamaterial,” *Applied Acoustics*, vol. 198, p. 108974, 2022.

[26] H. Duan, X. Shen, E. Wang, F. Yang, X. Zhang, and Q. Yin, “Acoustic multi-layer helmholtz resonance metamaterials with multiple adjustable absorption peaks,” *Applied Physics Letters*, vol. 118, no. 24, 2021.

[27] X. Yang, X. Shen, F. Yang, Z. Yin, F. Yang, Q. Yang, C. Shen, M. Xu, and J. Wan, “Acoustic metamaterials of modular nested helmholtz resonators with multiple tunable absorption peaks,” *Applied Acoustics*, vol. 213, p. 109647, 2023.

[28] Z. Liu, X. Zhang, Y. Mao, Y. Y. Zhu, Z. Yang, C. T. Chan, and P. Sheng, “Locally resonant sonic materials,” *American Association for the Advancement of Science*, vol. 289, no. 5485, pp. 1734–1736, 2000.

[29] J. Liu, H. Guo, and T. Wang, “A review of acoustic metamaterials and phononic crystals,” *Crystals*, vol. 10, no. 4, p. 305, 2020.

[30] Z. Yang, J. Mei, M. Yang, N. Chan, and P. Sheng, “Membrane-type acoustic metamaterial with negative dynamic mass,” *Physical review letters*, vol. 101, no. 20, p. 204301, 2008.

[31] S. A. Cummer, J. Christensen, and A. Alù, “Controlling sound with acoustic metamaterials,” *Nature Reviews Materials*, vol. 1, no. 3, pp. 1–13, 2016.

[32] Z. Yang, H. M. Dai, N. Chan, G. Ma, and P. Sheng, “Acoustic metamaterial panels for sound attenuation in the 50–1000 hz regime,” *Applied Physics Letters*, vol. 96, no. 4, 2010.

[33] J. Mei, G. Ma, M. Yang, Z. Yang, W. Wen, and P. Sheng, "Dark acoustic metamaterials as super absorbers for low-frequency sound," *Nature communications*, vol. 3, no. 1, p. 756, 2012.

[34] G. Ma, M. Yang, S. Xiao, Z. Yang, and P. Sheng, "Acoustic metasurface with hybrid resonances," *Nature materials*, vol. 13, no. 9, pp. 873–878, 2014.

[35] J. Allard and N. Atalla, *Propagation of sound in porous media: modelling sound absorbing materials*. John Wiley & Sons, 2009.

[36] J.-H. Xu, X.-F. Zhu, D.-C. Chen, Q. Wei, and D.-J. Wu, "Broadband low-frequency acoustic absorber based on metaporous composite," *Chinese Physics B*, vol. 31, no. 6, p. 064301, 2022.

[37] H. Zhao, Y. Wang, D. Yu, H. Yang, J. Zhong, F. Wu, and J. Wen, "A double porosity material for low frequency sound absorption," *Composite Structures*, vol. 239, p. 111978, 2020.

[38] G. Ji and J. Huber, "Recent progress in acoustic metamaterials and active piezoelectric acoustic metamaterials-a review.," *Applied Materials*, vol. 26, p. 101260, 2022.

[39] F. Y. F. R. Guo J, Zhang X, "Reflected wave manipulation by inhomogeneous impedance via varying-depth acoustic liners.," *Journal of Applied Physics.*, vol. 123, p. 12317, May. 2018.

[40] J. K. S. H. J.-H. K. S.-H. L. Song, Kyungjun and T. Kim., "Directional reflective surface formed via gradient-impeding acoustic meta-surfaces.," *Journal of Applied Physics.*, p. 32300, 2016.

[41] L. H. X. X. M. P. M. T. N. R. M. Yang, Tao and J. Militký., "Sound absorption properties of natural fibers: A review.," *Sustainability 12*, no. 20, p. 8477, 2020.

[42] N. Voronina, "Acoustic properties of fibrous materials.," *Applied Acoustic*, pp. 165–174, 1994.

[43] M. E. Delany and E. N. Bazley., "Acoustical properties of fibrous absorbent materials.," *Applied Acoustic*, pp. 105–116, 1970.

[44] Y. Miki, "Acoustical properties of porous materials-modifications of delany-bazley models.," *Journal of the Acoustical Society of Japan (E) 11*, pp. 19–24, 1990.

[45] J. Allard and N. Atalla., *Propagation of sound in porous media: modelling sound absorbing materials*. John Wiley & Sons, 2009.

[46] N. D. J.-M. G. Doutres, Olivier and O. Dazel., "Validity of the limp model for porous materials: A criterion based on the biot theory.," *The Journal of the Acoustical Society of America 122*, pp. 2038–2048, 2007.

[47] C. W. . Z. Y. Liu, S., "Design optimization of porous fibrous material for maximizing absorption of sounds under set frequency bands.," *Applied Acoustics*, pp. 319–328, 2014.

[48] D. K. Wilson, "Simple relaxational models for the acoustical properties of porous media.," *Applied Acoustics*, pp. 171–188, 1997.

[49] . P. R. Olny, X., "Acoustical determination of the parameters governing thermal dissipation in porous media.," *The Journal of the Acoustical Society of America*, pp. 814–824, 2008.

[50] S. M. R. . D. G. A. Champoux, Y., "Air-based system for the measurement of porosity.," *The Journal of the Acoustical Society of America*, pp. 910–916, 1991.

[51] P. R. . S. F. Pilon, D., "Behavioral criterion quantifying the edge-constrained effects on foams in the standing wave tube.," *The Journal of the Acoustical Society of America*, pp. 1980–1987, 2003.

[52] T. P. R. P. L. . S. S. Gokulkumar, S., "Measuring methods of acoustic properties and influence of physical parameters on natural fibers: A review.," *Journal of Natural Fibers*, 2020.

[53] K. V. Horoshenkov, "A review of acoustical methods for porous material characterisation.," *Int. J. Acoust. Vib*, pp. 92–103, 2020.

[54] K. V. Horoshenkov, *L'absorption acoustique des materiaux poreux*. PhD thesis, Universitt du Maine, 1991.

[55] D. Lafarge, *Propagation du son dans les materiaux poreux a structure rigide satures par un gaz: definition de parametres geometriques; analogies tlectromagnetiques; temps de relaxation et thiorie universelle*. PhD thesis, Universitt du Maine, 1993.

[56] J. Z. X. H. Guosheng Ji, Yi Fang, "Porous labyrinthine acoustic metamaterials with high transmission loss property.," *J. Appl. Phys.*, vol. 125, no. 215110, 2019.

[57] Y. Li, Y. Yan, and Y. Peng, "Ultra-broadband sound absorption of a multiple-cavity metastructure with gradient thickness," *Applied Acoustics*, vol. 133, p. 108140, February 2023.

[58] M. Harris, J. Potgieter, S. Ray, R. Archer, and K. M. Arif, "Acrylonitrile butadiene styrene and polypropylene blend with enhanced thermal and mechanical properties for fused filament fabrication," *Materials*, vol. 12, p. 244167, December 2019.

[59] S. Doddamani, B. Shrivastava, and N. Kumar, “Comprehensive review on noise reducing materials for habitable spaces,” *Applied Science and Engineering Progress*, vol. 15, p. 5726, 2022.

[60] R. Kruzel, T. Dembiczak, and J. Wachowicz, “Optimization of spark plasma sintering technology by taguchi method in the production of a wide range of materials: Review,” *Materials*, vol. 16, p. 5539, 2023.

[61] R. S. Raman, N. Kukreja, and N. Singh, “Process parameters optimization through taguchi and anova analysis-a review,” in *IOP Conference Series: Materials Science and Engineering*, vol. 1116, p. 012090, IOP Publishing, April 2021.

[62] S. Sunardi, D. Ariawan, E. Surojo, A. R. Prabowo, H. I. Akbar, B. Cao, and H. Carvalho, “Assessment of eggshell-based material as a green-composite filler,” *Journal of the Mechanical Behavior of Materials*, vol. 32, no. 1, p. 20220269, 2023.

[63] G. Manickavasagam, M. Saaid, and V. Lim, “Impact of prolonged storage on quality assessment properties and constituents of honey: A systematic review,” *Journal of Food Science*, vol. 89, no. 2, pp. 811–833, 2024.

[64] T. Burger, “Controlling for false discoveries subsequently to large scale one-way anova testing in proteomics: Practical considerations,” *Proteomics*, vol. 23, no. 18, p. 2200406, 2023.

[65] C. Marescotti and F. Pompoli, “Geometric optimisation of a multiple coiled up resonator for broadband and octave band acoustic absorption,” *Applied Acoustics*, vol. 221, p. 110000, 2024.

[66] D. M. Garza-Agudelo, V. C. Henriquez, C.-H. Jeong, P. R. Andersen, M. Ibarias, J. Sanchez-Dehesa, and F. Lucklum, “Metasurfaces for sound absorption over a

broad range of wave incidence angles," *Applied Acoustics*, vol. 220, p. 109965, 2024.

[67] G. do N. Almeida, E. F. Vergara, L. R. Barbosa, and R. Brum, "Low-frequency sound absorption of a metamaterial with symmetrical-coiled-up spaces," *Applied Acoustics*, vol. 172, p. 107593, 2021.